

## **Physical and theoretical modeling of rock slopes against block-flexure toppling failure**

Mehdi Amini<sup>1\*</sup>, Mohammad Gholamzadeh<sup>2</sup> and Mohammad Hossein Khosravi<sup>1</sup>

*1. School of Mining Engineering, College of Engineering, University of Tehran, Iran*

*2. Msc Student, Department of Mining Engineering, University of Kashan, Iran*

Received 7 Sep. 2015; Received in revised form 14 Oct. 2015; Accepted 18 Oct. 2015

*\* Corresponding Author Email: mamini@ut.ac.ir, Phone, fax: +98-21-88008838*

### **Abstract**

Block-flexure is the most common mode of toppling failure in natural and excavated rock slopes. In such failure, some rock blocks break due to tensile stresses and some overturn under their own weights and then all of them topple together. In this paper, first, a brief review of previous studies on toppling failures is presented. Then, the physical and mechanical properties of experimental modeling materials are summarized. Next, the physical modeling results of rock slopes with the potential of block-flexural toppling failures are explained and a new analytical solution is proposed for the stability analysis of such slopes. The results of this method are compared with the outcomes of the experiments. The comparative studies show that the proposed analytical approach is appropriate for the stability analysis of rock slopes against block-flexure toppling failure. Finally, a real case study is used for the practical verification of the suggested method.

**Keywords:** *analytical solution, blocky-flexure toppling failure, case study, physical modeling.*

### **1. Introduction**

Toppling failure is one of the most probable instabilities of layered rock slopes. The failure was first mentioned by Müller after studying the instabilities near the "Vaiont" dam lake in 1968[1]. In 1971, based on theoretical and physical modeling, Ashby proposed the term "toppling" for such failures [2]. In 1976, Goodman and Bray classified the toppling failures into four principal types: flexural, blocky, block-flexure, and secondary. Also, they suggested an analytical approach for the

stability analysis of slopes against block toppling failure on the basis of a step-by-step method. This approach presented many times for the analysis of block toppling failures in the form of design charts and computer programs [3-6]. After 1986, based on Goodman and Bray's classification, numerous researches were carried out on blocky and flexural toppling failures [7-20]. Aydan and Kawamoto were the first to propose a complete theoretical solution to analyze slopes

and underground openings prone to flexural toppling failures, on the basis of a limiting equilibrium method utilizing the bending theory of cantilever beam with the consideration of gravity, earthquake, and water pressure [10]. Adhikary et al. (1997, 2007) presented a numerical method for the analysis of the failure based on the Cosserat approach and centrifuge physical modeling [14]. In addition, Amini et al. (2008) proposed a procedure to determine the safety factor of rock slopes against flexural toppling failure on the basis of the deflection compatibility of rock columns [15, 16]. In 2009, Brideau and Stead carried out a study on some numerical three-dimensional models with a potential of toppling failures and explained their results [21]. As it can be seen in the literature, researches on toppling failures have concentrated mostly on blocky and flexural types. However, rock is a natural material and its discontinuities are generally irregular; therefore, pure toppling failures (flexural and blocky) are infrequent and most of such failures, occurring in layered natural rock

slopes, are of block-flexure type (Fig. 1). In 2010, Amini et al. presented an analytical method for evaluating rock slopes against block-flexure toppling failure based on Aydan-Kawamoto and Goodman-Bray approaches [18]. In 2014, Mohtarami et al. studied the interaction between soil and rock blocks and presented a new analytical solution for combined circular-toppling failure [22]. Also, in 2014, Amini et al. described the stability analysis of rock slopes facing dam lakes against block toppling failure on the basis of theoretical models and a real case study [23]. Recent studies on this field can be found in the works of Alejano et al. in 2015 [24]. They modelled toppling failures with rounded edge rock blocks and presented some new theoretical and experimental considerations for their assessments.

In the current study, the failure is modeled in laboratory with tilting table apparatus and its mechanism is assessed. Consequently, a new analytical approach is suggested to evaluate rock slopes against such failure.

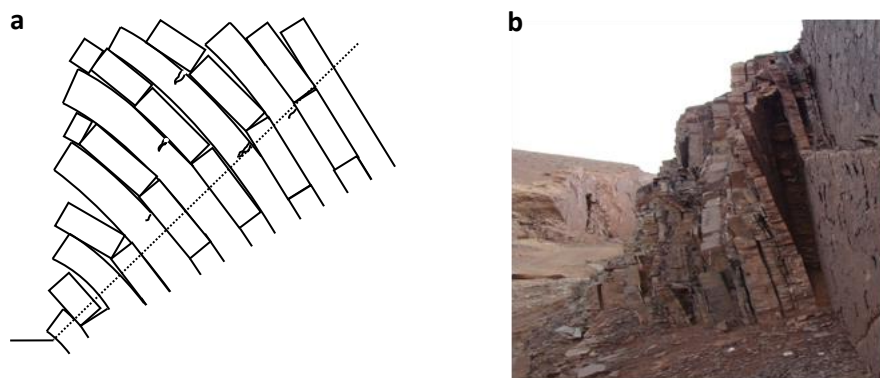


Fig. 1. Block-flexural toppling failure in rock slopes, a) schematic diagram, b) actual case study (north slope of the "Venarch" mine, Iran)

## 2. Physical modeling of block-flexure toppling failure

Evaluating the behavior of natural rock slopes is complicated; therefore, the mechanism of their probable instabilities is sometimes studied through ideal physical modeling. However, the latter is quite time-consuming and costly, and the selection of the proper materials for the models needs high precision. Effort has been made in this research to evaluate the block-flexure toppling failure

mechanism using physical modeling explained briefly in the following sections.

### 2.1. Physical and mechanical properties of the materials

2800 gr of a special chemical powder has been used to prepare one sample block. This powder was a mixture of some chemicals and Vaseline oil, with specified proportions, mixed thoroughly and compacted in a steel mold of 50×5×6 cm under a consolidation pressure of

210 kPa. Under this pressure, the powder particles stick together thoroughly and form solid blocks (Fig. 2). Using these blocks, it is possible to construct a variety of blocky and layered rock slopes. The powder composition is such that the resulted blocks have high densities and low tensile strengths; therefore, they may break under their weights even with

small dimensions. Although such blocks have been used several times by other researchers and have undergone several tests [9, 10, 17, 21], in the present study, the physical and mechanical properties of the blocks were retested in the laboratory. The test procedures and their final results will be explained in detail in the following sections.



**Fig. 2. Material used for physical modeling, before and after consolidation**

### **2.1.1. Unit weight**

The blocks' unit weights depend much on the consolidation pressure; the more the pressure is, the more the materials are consolidated. In the present study, the powder weight in the mold was 2800 gr resulting in a 50×5×4.7 cm block with a unit weight of 23.4 kN/m<sup>2</sup>.

### **2.1.2. Uniaxial compressive strength**

A key mechanical property of a block needed to make decisions regarding the construction of a physical model is the uniaxial compressive strength. To determine this parameter, the total number of seven 10×5×4.7 cm blocks were selected and tested randomly (Fig. 3). Figure 4 shows the stress-strain curves of these tests. As shown in the figure, the uniaxial compressive strength of these blocks varies between 45 and 65 kPa, but the average value is nearly 56.7 kPa (Fig. 5).



**Fig. 3. Determination of the uniaxial compressive strength of the solid blocks**

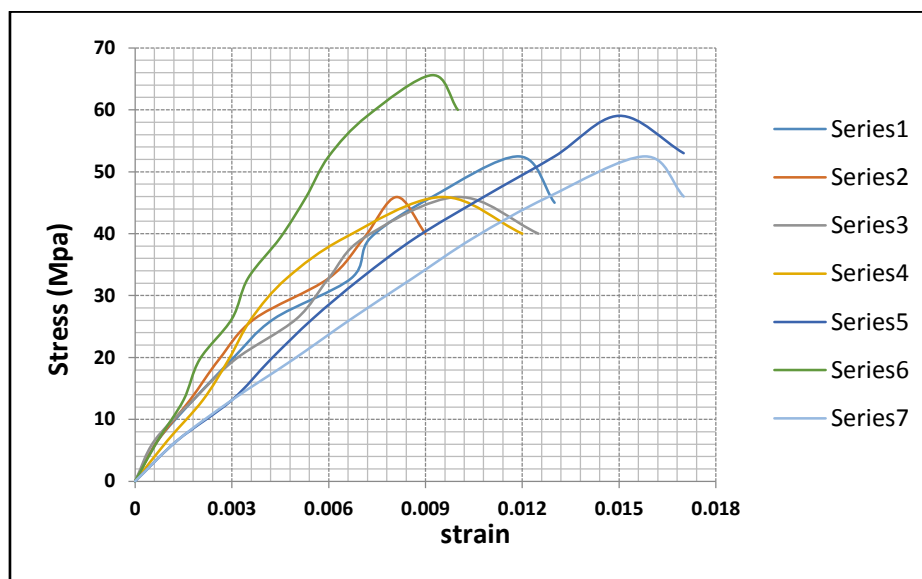


Fig. 4. Stress-strain curves of the uniaxial compressive strength tests

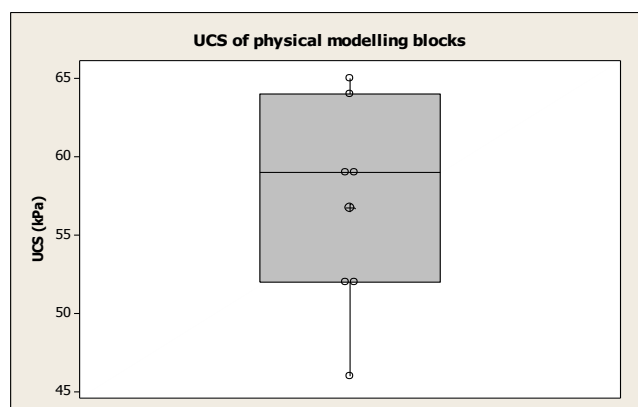


Fig. 5. Box plot of the uniaxial compressive strength tests results

### 2.1.3. Modulus of elasticity

The elasticity modulus can be determined through finding the gradients of the stress-strain curves drawn based on the results of the uniaxial compressive strength tests. Using Figure 4, the elasticity moduli of the tested blocks were found to be 3.3 -7.1 MPa.

### 2.1.4. Tensile strength

The stability of the models with the potential of block-flexure toppling failure is very sensitive to the tensile strength of the blocks. On the other hand, since these blocks are quite weak against tensile stress, it is not possible to easily estimate their tensile strength through such conventional methods as the “Direct Tension”, “Brazilian”, or “Point Load”. Other researchers have used three- or four-point bending tests wherein the failure may also

occur in the supports and cause errors in the test results. Therefore, in the present research, to determine the more reliable tensile strength, a special apparatus was designed and constructed in which a block more than 20 cm long lies on a small conveyer belt at the end of which a balance weight is placed on the block (Fig. 6). When the motor starts, the belt moves causing one end of the block to exit; under such conditions, the block behaves like a cantilever beam. As time passes, the beam's effective length increases and the block suddenly breaks under its own weight and the laser transducer in the apparatus registers the time of the block failure. Various tests have shown that the blocks in this research break at an effective length of 14.5 cm; therefore, having this length and the blocks densities,

their tensile strength can be obtained as follows:

$$\sigma_t = \frac{My}{I} = \frac{w \cdot \frac{h}{2} \cdot \frac{t}{2}}{\frac{1}{12}bt^3} = \frac{b \cdot t \cdot h \cdot \gamma \cdot \frac{h}{2} \cdot \frac{t}{2}}{\frac{1}{12}bt^3} \quad (1)$$

$$= \frac{3h^2\gamma}{t} = \frac{3 \times 14.5^2 \times 10^{-4} \times 23.3}{4.7 \times 10^{-2}}$$

$$= 31.37 \text{ kPa}$$

where the parameters which have been used in the equation are:  $M$ : bending moment,  $I$ : Moment of inertia,  $y$ : Distance from neutral axis,  $w$ : Weight of the column,  $h$ : Effective length of the column,  $t$ : Thickness of the column.

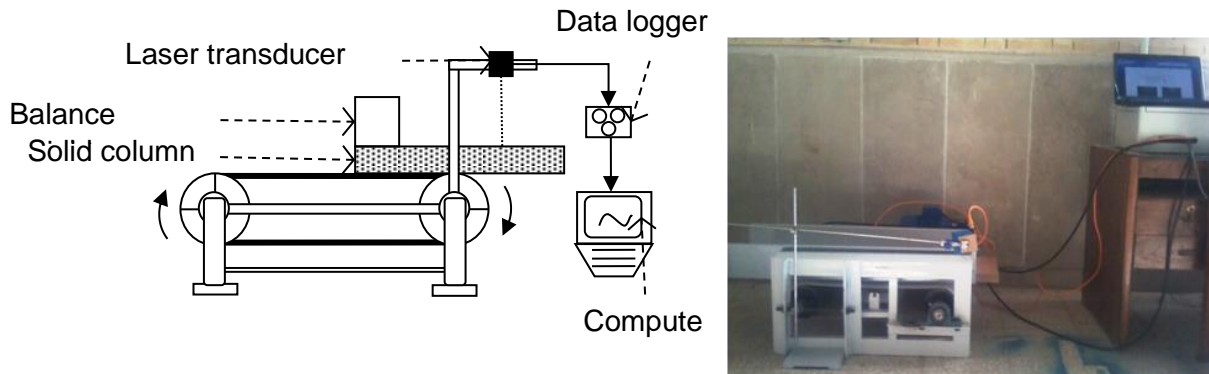


Fig. 6. Tensile strength determination of solid blocks with a new apparatus

## 2.2. Tilting table apparatus

One way of evaluating the results of theoretical analyses is testing the physical models in the laboratory [22]. Tilting table, base friction, and centrifuge are among the common geotechnical methods used for the examination of the behavior of scaled soil and rock structures. In this research, a tilting table (Fig. 7) was constructed to study the mechanism of the block-flexure toppling failure. It has a box (90 cm long, 60 cm wide, and 50 cm high) placed over a pneumatic jack to set up the models. The jack gradually increases the table angle, and the dip of the blocks and the slope angle vary proportionately. Other components in the tilting table include the compressed air compressor, air-transfer hoses, compressed air fittings and fasteners, the table's angular velocity control equipment, and devices used to read the table slope and laser transducer. After the model is set up, the table is tilted until failure occurs. On this basis, the angle at

which the model starts to fail or slide can be considered as the angle of instability.

## 2.3. Two-block physical modeling

Before constructing the main model, we first made some two-block models that had the potential of block-flexure toppling failure and studied their failure behavior. Since this failure modeling was done for the first time and there existed no previous related experiences, we obtained excellent experience in a short time and with low costs, and it enabled us to better select the dimensions of the main model. To make two-block models, two blocks were set up on the table: one in the front as a cantilever beam (with the potential of flexural toppling failure) and the other, with the same height and a free end, behind it (with the potential of block toppling failure). The table was, then, tilted until failure occurred (Fig. 8), and the table angle was measured at the moment of toppling. The test was repeated for 10-25cm-long blocks. The results are given in Table 1.

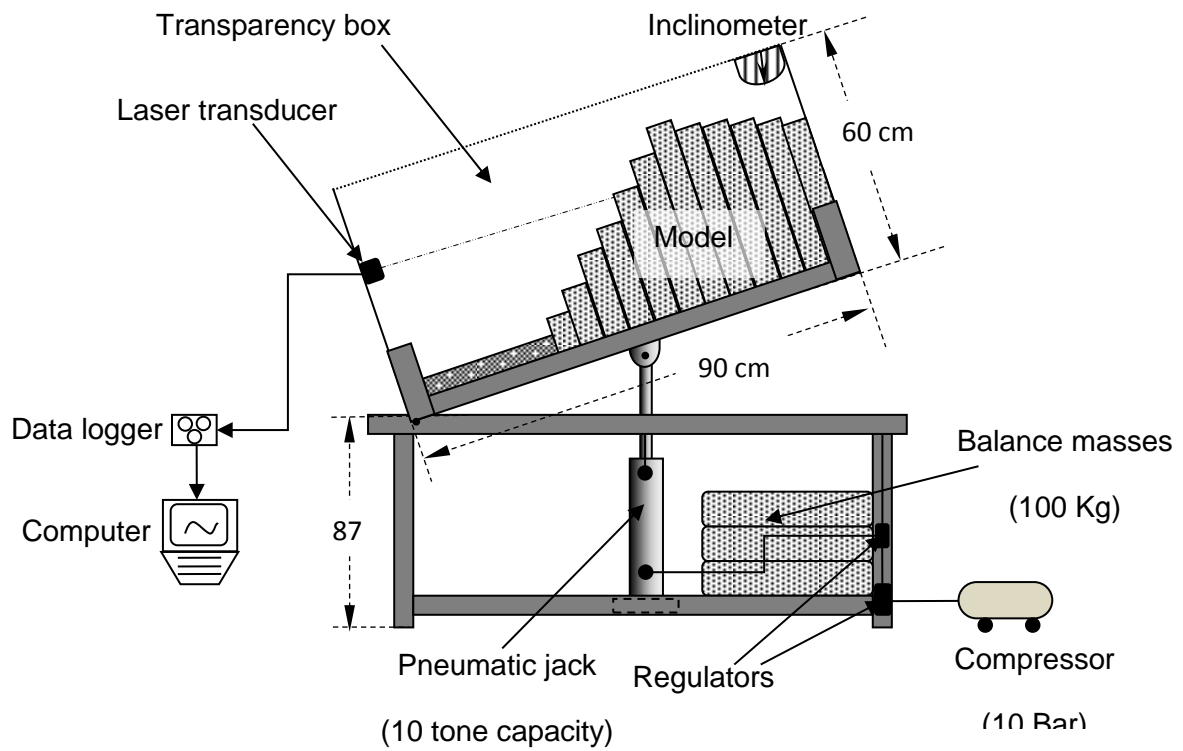


Fig. 7. Tilting table



Fig. 8. Physical modeling of two-blocks with a potential of block-flexural toppling failure

**Table 1. Results of two-block physical modeling**

| No. | Effective length (cm) | Table inclination (°) |
|-----|-----------------------|-----------------------|
| 1   | 10                    | 58                    |
| 2   | 15                    | 31                    |
| 3   | 20                    | 20                    |
| 4   | 25                    | 15                    |

**3. Theoretical modeling of two blocks with the potential of block-flexure toppling failure**

Figure 9 shows the schematic view of a theoretical two-block model with the potential of block-flexure toppling failure. At the time of failure, block 2 with the potential of toppling, sliding, or toppling-sliding, exerts a special distributed force (with a uniform-to-triangular pattern) on the adjacent column. This column has a potential of flexural toppling failure and carries a tensile stress at its pivot. If the maximum resultant tensile stress produced at the pivot is greater than the tensile strength of the materials, the column cracks and the model becomes unstable. Since equilibrium occurs simultaneously in the entire system and in its individual components, it may be assumed that system’s factor of safety is related to those of the individual components. If it is assumed that the system’s factor of safety is equal to the linear combination of the factor of safety of each of the individual components, we can find the two-block model safety factor against block-flexure toppling failure as follows:

$$F_{SBF} = aF_{SB} + bF_{SF} \tag{2}$$

where  $F_{SF}$  is the safety factor of block 1 against flexural toppling failure and  $F_{SB}$  is the safety factor of block 2 against blocky toppling failure. If a block with a potential of flexural toppling failure is modelled with a cantilever beam and a block with a potential of blocky toppling failure is modelled with a beam-column,  $F_{SB}$  and  $F_{SF}$  are found through limit equilibrium equations and substituted in Equation (2). We will then have:

$$F_{SBF} = \frac{at}{h \cdot \tan \delta} + \frac{b \cdot t \cdot \sigma_t}{3h^2 \cdot \gamma \cdot \cos \delta} \tag{3}$$

where  $\delta$  is the angle of solid blocks with the horizon and  $\sigma_t$  is the tensile strength of these blocks.

If, in Equation (3), both blocks are capable of pure blocky toppling failure, then  $a=1$  and  $b=0$ , and if they both have the potential of pure flexural toppling failure, then  $a=0$  and  $b=1$ ; therefore, the boundary conditions of Equation (3) can be found through these values. If the physical and mechanical properties of the blocks and the boundary values of “a” and “b” are substituted in Equation (3), we can draw the graphs of the blocks’ effective lengths versus the table angle under the limit equilibrium condition. These graphs show the upper and lower boundaries of the block-flexure toppling failures; therefore, the zone between the two shows the failure zone (Fig. 10). In this failure zone, “a” and “b” show the rate of the tendency of the block-flexure toppling failure compared with the ideal (pure blocky and flexural toppling) failures. Next, we will suggest appropriate values for “a” and “b” using the physical modeling results.

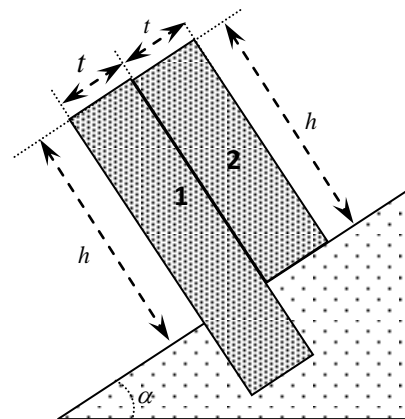


**Fig. 9. Theoretical model for two blocks with the potential of block-flexure toppling failure**

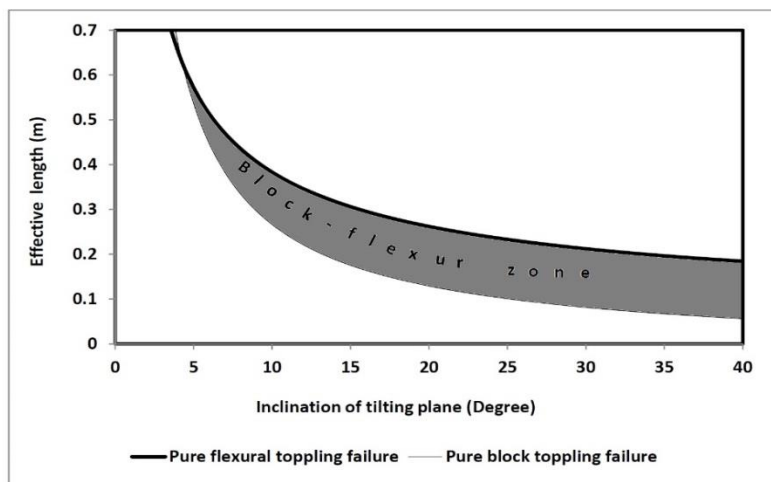


Fig. 10. Block-flexure toppling failure zone for two-block models

#### 4. Comparison of the theoretical and physical modeling results for the two-block model

To validate the results of the proposed theoretical approach for the analysis of two-block models against block-flexure toppling failure and determine “a” and “b” values, the model results were compared with those of the physical modeling (Fig. 11). To better interpret the graphs, the pure blocky and flexural toppling failure boundaries have been shown, too. As shown, for a two-block case where one block with a blocky toppling failure potential lies on one with a flexural toppling failure potential, if “a” and “b” values are assumed as 0.5, the theoretical and laboratory results will have the best conformity. This figure also shows the desirable conformity of the results at the boundaries. Totally, this

comparison concludes that “a” and “b” can be found as follows:

$$a = \frac{m}{m+n}, \quad b = \frac{n}{m+n} \quad (4)$$

where “m” and “n” are the number of blocks with the potential of blocky and flexural toppling failure, respectively. Therefore, the relation between “a” and “b” can be found as follows:

$$a = (1 - b) \quad (5)$$

Substituting Equation (5) in Equation (3), we can find the final equation for the determination of the factor of safety of the block-flexure toppling failure for some equal-height blocks as follows:

$$F_{SBF} = a \frac{t}{h \cdot \tan \delta} + (1 - a) \frac{t \cdot \sigma_t}{3h^2 \cdot \gamma \cdot \cos \delta} \quad (6)$$

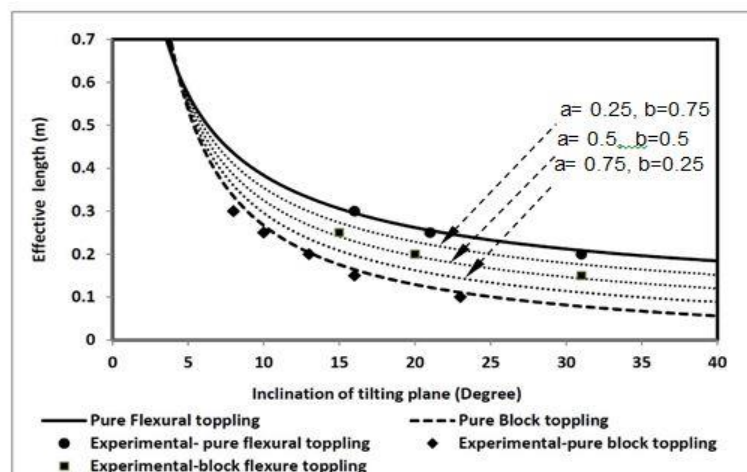


Fig. 11. Comparison between theoretical and experimental results



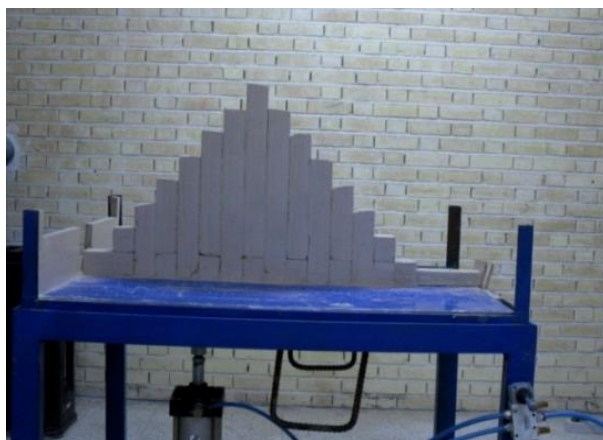
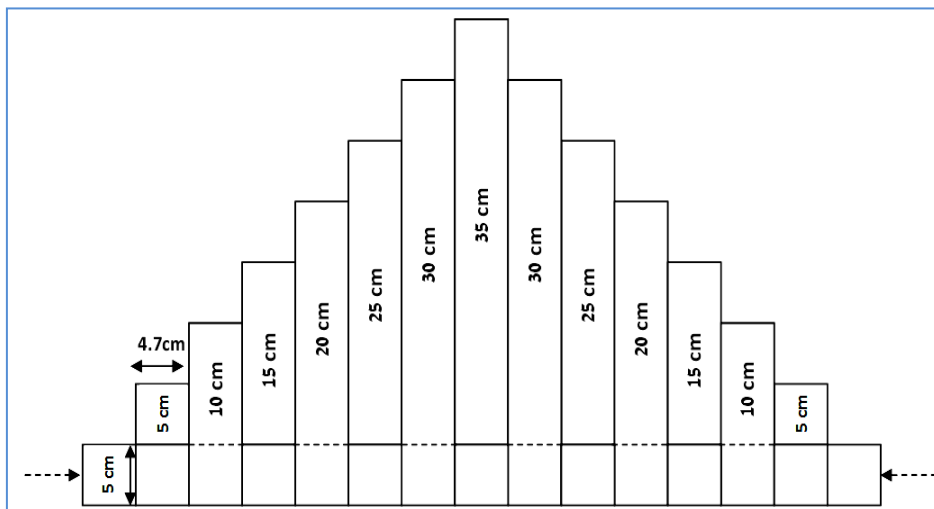
**5. Modeling rock slopes against block-flexure toppling failure**

After presenting a theoretical model for the analyses of two-block failures, we modeled rock slopes with the potential of block-flexure toppling failure in two series: first, it was assumed, quite ideally, that the slope's block geometries are divided into two blocky and flexural parts so that every other block is potentially blocky or flexural. These models are, of course, quite different from real rock slopes because, in nature, slope blocks are usually arranged quite randomly; therefore, in the second series, we followed the same pattern (random arrangement) so as to show more similarity with real naturally layered rock slopes. In both series, after the models were constructed, the table was tilted gradually to cause the failure to occur. At the moment of failure, such parameters as the

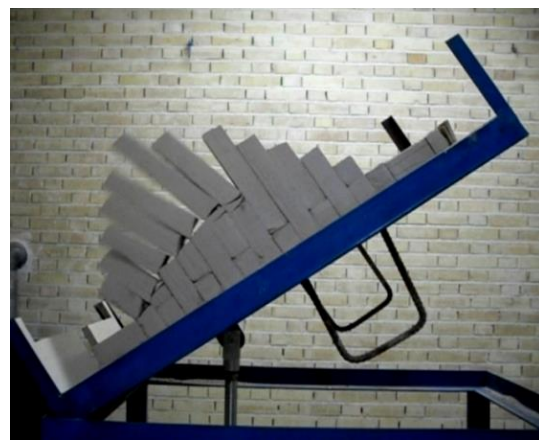
table angle, total failure plane angle, and so on were measured. In what follows, we will explain the two modeling sets separately.

**5.1. Ideal block-flexure toppling failure modeling**

Figure 12 shows an example of such modeling before the test and after failure; in these models, the blocks regularly undergo blocky and flexural failures. In fact, every consecutive two blocks resemble the two-block models; one block is fixed at its pivot and is capable of carrying tensile stresses, but the next block is free at its end and imposes its weight, after the table tilts, on the fixed block. Because of some limitations regarding the construction and placement of the blocks, the heights of the slopes vary from 41 to 47.39 cm. Table 2 shows the modeling results.



a)



b)

**Fig. 12. Ideal block-flexure toppling failure modeling**

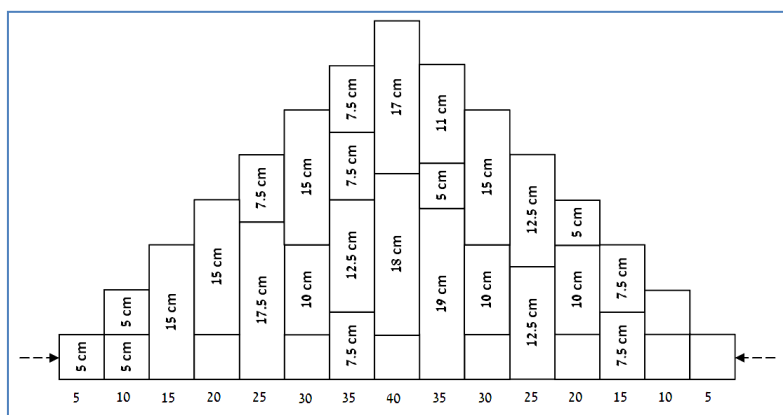
**Table 2. Geometrical parameters of rock slope models having a potential of block-flexure toppling failure with ideal setup**

| No. | $\beta$ ( $^{\circ}$ ) | $\varphi$ ( $^{\circ}$ ) | $\delta$ ( $^{\circ}$ ) | $\theta$ ( $^{\circ}$ ) | H (cm) |
|-----|------------------------|--------------------------|-------------------------|-------------------------|--------|
| 1   | -12                    | 18                       | 57                      | 102                     | 53.49  |
| 2   | -8                     | 15                       | 55                      | 98                      | 47.39  |
| 3   | -2                     | 12                       | 47                      | 92                      | 44.24  |

**5.2. Modeling block-flexure toppling failure with random setup**

In the second series, the blocks were placed in the model quite randomly so that some blocks could break and some could overturn freely. The length of these blocks was selected

between 5 to 20 centimeters. When the length of all blocks is 5 centimeters, blocky toppling failure occurs, because blocks can overturn freely. Also, when all the blocks are continuous, we have flexural toppling failure. Our experiments showed that if the length of the blocks are selected randomly, the models fail due to block-flexure toppling failures. The models' heights were considered to be approximately 45 cm so that the inclination of rock slope may not exceed  $90^{\circ}$  at the failure time. Fig. 13 shows the schematic view and two photos of a model selected from these experiments. All modeling results are given in Table 3.



a)



b)

**Fig. 13. Physical modeling of rock slopes against block-flexure toppling**

**Table 3. Geometrical parameters of the physical models of rock slopes having a potential of block-flexural toppling failure with random setup**

| No. | $\beta$ ( $^{\circ}$ ) | $\varphi$ ( $^{\circ}$ ) | $\delta$ ( $^{\circ}$ ) | $\theta$ ( $^{\circ}$ ) | H (cm) |
|-----|------------------------|--------------------------|-------------------------|-------------------------|--------|
| 1   | -24                    | 17                       | 67                      | 110                     | 44.97  |
| 2   | -16                    | 27                       | 59                      | 102                     | 46.81  |
| 3   | -10                    | 29                       | 53                      | 96                      | 47.59  |
| 4   | -24                    | 21                       | 67                      | 110                     | 44.97  |
| 5   | -20                    | 15                       | 63                      | 106                     | 47     |
| 6   | -28                    | 14                       | 71                      | 114                     | 43.72  |

**6. Analysis of block-flexural toppling failure**

In 2008, Amini et al. presented a theoretical method for the analysis of the pure flexural toppling failure [15]. This method's authenticity was confirmed through comparing its results with those of the "Centrifuge", "Base Friction", "Tilting Table", and "Shaking Table" modeling methods. According to the presented method, a rock column safety factor against flexural toppling failure can be assumed equal to that of a single cantilever

beam. The thickness, inclination, and all the other physical and mechanical properties of such a beam are exactly the same as those of rock columns in a rock slope, and its length is found from Equation (7). This approach is known as the “Equivalent Length” method. It is worth mentioning that in the original paper, the upper surface of the rock slope has been assumed to be horizontal, but in the present study the principal equations have somewhat changed and have become more generalized, because according to the following relations, the upper surface of a slope can lie below or above the horizontal plane.

$$A = \frac{\tan(\delta - \varphi \pm \beta) \cos^2 \varphi}{\tan(\delta - \varphi \pm \beta) + \tan(\theta - \delta + \varphi)} \quad (7)$$

$$B = \frac{2 \cos(\theta - \delta + \varphi) \cos \varphi}{\sin \theta} H \quad (7-1)$$

$$C = \left[ \frac{\cos(\theta - \delta + \varphi)}{\sin \theta} H \right]^2 \quad (7-2)$$

$$\psi = \frac{-B \pm (B^2 - 4AC)^{0.5}}{2A} \quad (7-3)$$

where the parameters which have been used in the equation are:  $\psi$ : equivalent length of rock slope,  $\delta$ : Angle of rock mass stratification with respect to the horizontal,  $\varphi$ : Angle between total failure plane and the line of normal to discontinuities,  $\theta$ : Angle between face slope with respect to the horizontal,  $\beta$ : Angle of upper surface of rock slope with respect to the horizontal,  $H$ : slope height. These parameters have been shown in Figure 14.

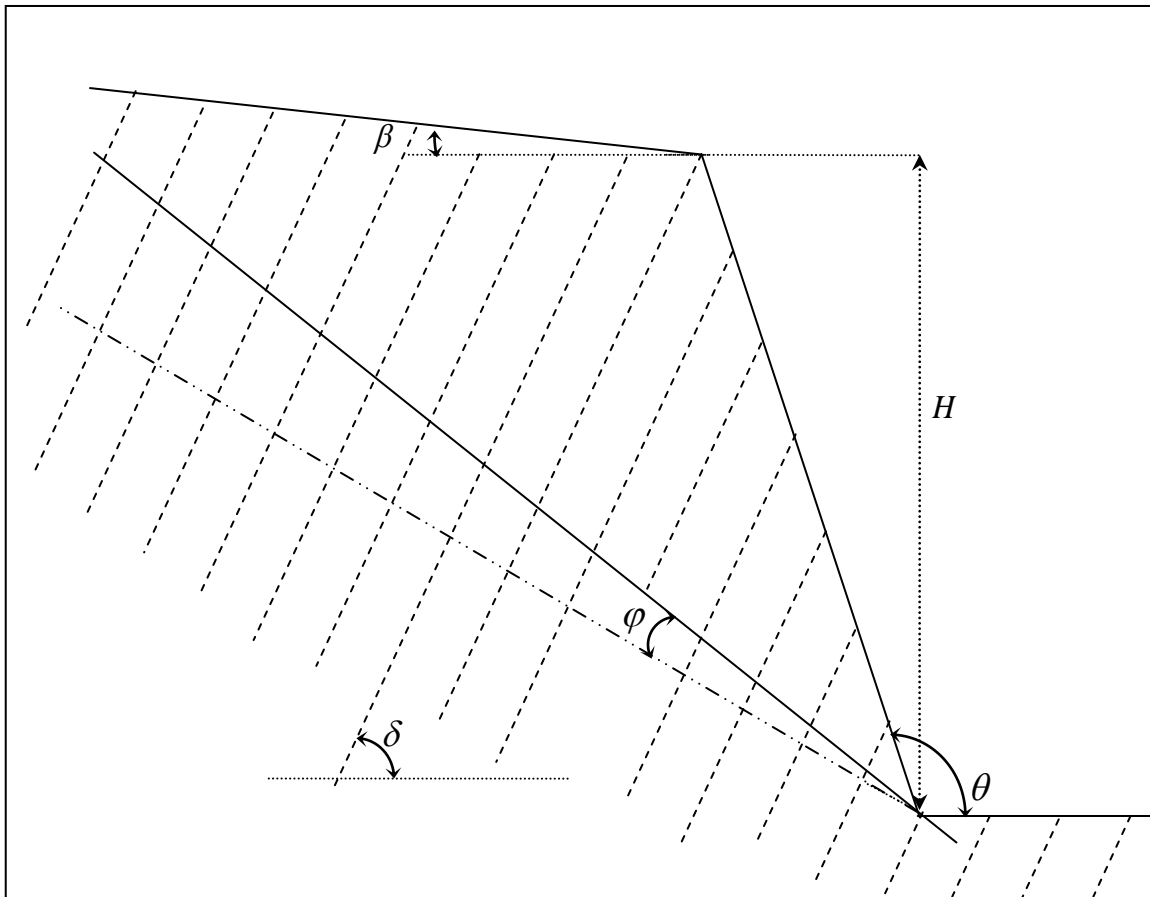


Fig. 14. Schematic picture of a rock slope with a potential of toppling failure

Therefore, the factor of safety against the flexural toppling failure can be found as follows [15]:

$$F_s = \frac{t \cdot \sigma_t}{3\psi^2 \cdot \gamma \cdot \cos \delta} \quad (8)$$

Also, the safety factor of a block with length  $\psi$  against block toppling failure is found as follows:

$$F_s = \frac{t}{\psi \cdot \tan \delta} \quad (9)$$

As mentioned earlier for two-block models, in block-flexure toppling failures, the blocks with toppling failure potentials exert part of their weight force on the cantilever rock column. On this basis, it is suggested that, for the analyses of rock slopes against block-flexure toppling failures, a combination of the above relations be used as follows:

$$F_{SBF} = k \frac{t}{\psi \cdot \tan \delta} + (1-k) \frac{t \cdot \sigma_t}{3\psi^2 \cdot \gamma \cdot \cos \delta} \quad (10)$$

where  $k$  is a dimensionless modification factor varying between 0 and 1; this factor shows the percentage of blocks with a pure blocky potential compared to the total blocks in the rock slope. If all the blocks in a slope are cantilevers under flexure, the slope will be capable of a pure flexural toppling failure and this factor will be 0; otherwise, it will be less than 1. Also, if all the blocks in a slope have blocky potentials, the factor will equal 1 and the failure will be of a pure blocky toppling type.

### 7. Comparison between theoretical and experimental results

In the previous section, Equation (10) was proposed for the determination of the rock slope safety factor against block-flexure toppling failure. At the moment of failure, the slope factor of safety against the failure is 1; therefore, it is possible, using the experiments in this research, to validate the results of the suggested approach. For more clarifications, we also made some physical models with the potentials of pure blocky and flexural toppling failures through which it is possible to evaluate the boundary conditions ( $k=0$  and  $1$ ) of Equation (10). The physical and theoretical modeling results have been compared in Figure 15. As shown, under limit conditions, there is relatively good conformity between the experimental results and those of Equation

(10). The error of this relation is, of course, more than those of two-block models, because in this case, the models' conditions are more complicated. In this figure, the graph found for Equation (10) has also been drawn for  $k=0.5$ . As shown, this graph thoroughly conforms to the results of the ideal models of block-flexure toppling failures. In these models, the number of blocks with pure blocky failure potentials is equal to that of those with pure flexural failure potentials, and the failure plane is such that half of the blocks have failed due to the tensile stresses. However, in non-ideal models, since the blocks are placed randomly, the failure plane is so formed that fewer blocks break. Therefore, in most of these models, the experimental results are between the blocky and ideal block-flexure curves. This comparison shows that Equation (7) can be used to analyze and predict the rock slope behavior against block-flexure toppling failure.

### 8. Analysis of a real case study with the proposed approach

In the previous section, a new theoretical model was proposed for the analyses of block-flexure toppling failures. The comparison of the results of this model with those found from experimental modeling showed that the suggested approach was satisfactorily precise and correct. Since the ultimate goal of such methods is to analyze the stability of real rock slopes that have the potential of block-flexure toppling failure, it is necessary that their results be compared with those found from case study examples. In this section, a real rock slope with a block-flexure toppling failure potential has been analyzed, using the theoretical method proposed in this paper, and the results have been compared.

#### 8.1. Rock slope features

"Chaloos" is the road that connects Tehran to the north of Iran. A major part of its bed has been constructed through excavating trenches in layered sandstone. The rock slope facing this road in km 55.4 has a potential of block-flexure toppling failure (Fig. 16). The rock mass of this slope is made of thick layers of sandstone. The geometrical specifications of the rock slope and the rock mass discontinuities were gathered through field observations and studied using the

DIPS software. Figure 17 shows the results of the investigations. As shown, there are two sets of dominating discontinuities in the rock mass: a set of joints and a bedding plane; the persistence of the bedding plane is such that it can be observed regularly throughout the rock mass, but the joints' persistence is, at most, equal to the thickness of the rock mass layers so that they do not cover the whole rock mass continuously. To determine the geo-mechanical properties of the rock mass, some rock blocks were taken from the site and transferred to the laboratory. In the

laboratory, many cores were obtained from the rock blocks and tested.

Tables 4, 5, and 6 show the physical and mechanical results of the tests performed on the core samples. In addition, in order to evaluate the overall characteristics of the rock slope, its rock mass was classified based on the GSI and RMR approach; on these bases, the rock mass RMR was 40-45 and its GSI was 30-35. The rock mass specifications, considering engineering classifications, were determined and are shown in Table 7.

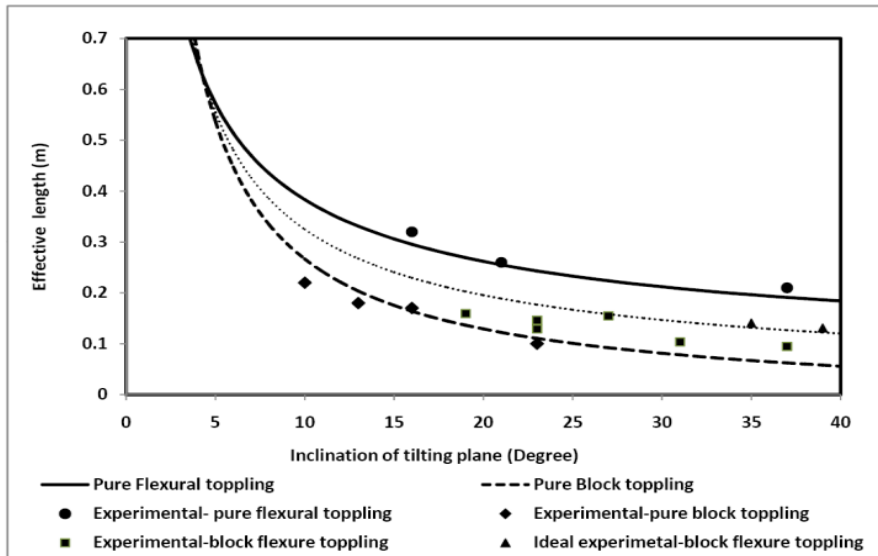


Fig. 15. Comparison between theoretical and experimental results

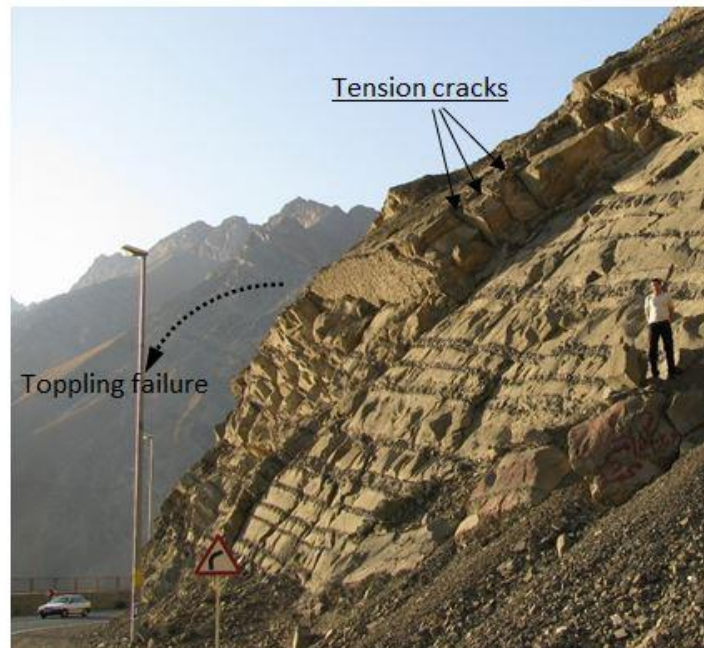


Fig. 16. Block-flexural toppling failure in “Chaloos” road (km 55.4)

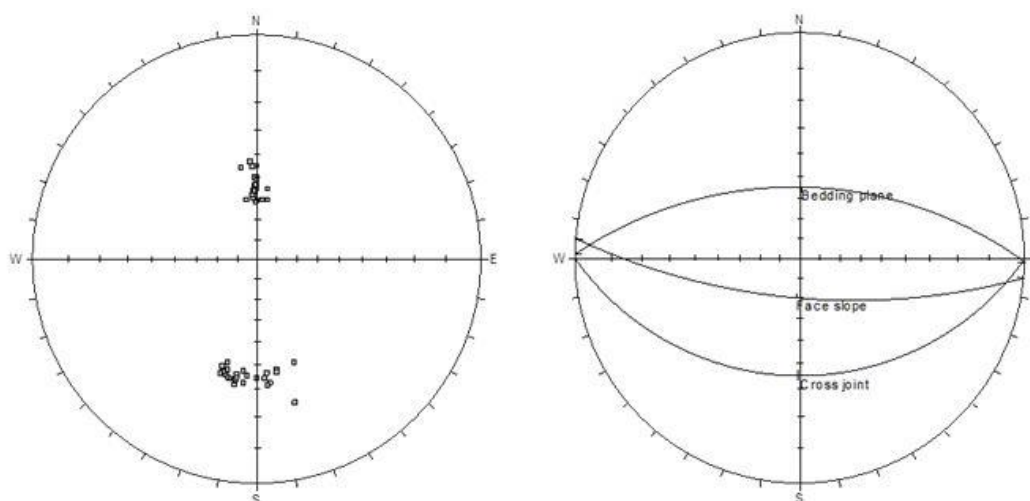


Fig. 17. Stereonet diagrams of discontinuities and the face slope of the case study

Table 4. Physical properties of Sandstone samples

| Rock Type | Physical Properties           |     |            |                    | Point Load | Durability Index |
|-----------|-------------------------------|-----|------------|--------------------|------------|------------------|
|           | Density (gr/cm <sup>3</sup> ) |     | Porosity % | Water Absorption % | Is (50)    |                  |
|           | Dry                           | Sat |            |                    |            |                  |
| Sandstone | 2.3                           | 2.5 | 1.4        | 1                  | 1.5        | 98               |

Table 5. Geomechanical properties of Sandstone samples

| Rock Type | Uniaxial compressive strength test |        | Brazilian        | Sound velocity |      |         |      |
|-----------|------------------------------------|--------|------------------|----------------|------|---------|------|
|           | $\sigma_c$ (MPa)                   | E(GPa) | $\sigma_t$ (MPa) | Vp(m/s)        |      | Vs(m/s) |      |
|           | Sat                                | Sat    | Sat              | Dry            | Sat  | Dry     | Sat  |
|           | Sandstone                          | 26     | 11               | 2.3            | 5650 | 5680    | 2690 |

Table 6. Shear strength parameters of Sandstone samples

| Rock Type | Tri-axial Compressive Strength Test |        |                  |   | Direct Shear Test |        |         |        |
|-----------|-------------------------------------|--------|------------------|---|-------------------|--------|---------|--------|
|           | c (MPa)                             | $\Phi$ | Hoek's Constants |   | Residual          |        | Peak    |        |
|           |                                     |        | $m_i$            | S | c (MPa)           | $\phi$ | c (MPa) | $\phi$ |
|           |                                     |        |                  |   |                   |        |         |        |

Table 7. Specification of the rock mass of the case study

| $m_b$ | s      | A     | c (MPa) | $\phi^\circ$ | $E_m$ (GPa) | $\sigma$ (MPa) |
|-------|--------|-------|---------|--------------|-------------|----------------|
| 0.21  | 0.0001 | 0.518 | 0.299   | 25.62        | 5.336       | 0.196          |

### 8.2. Stability analysis of the case study slope

To analyze the stability of this slope, we first studied its stability using stereographic diagrams; the results are shown in Fig. 18. As

shown, the poles of the rock mass cross-joints are in the plane failure zone, and those of its bedding planes are in the toppling failure region. Since the joints are not fully continuous, there will not be any potential of

complete plane failure and the rock mass has only a potential of block-flexure toppling failure. Also, site investigation shows that, in this case, some rock blocks fail due to bending tensile stresses, and some blocks overturn due to their own weights, and overall block-flexural toppling failure occurs. Hence, the

theoretical method that is presented in this paper can be used to assess the slope.

To find the safety factor of this slope against toppling failure based on the method proposed in this paper, the parameters required for Equations (7) and (10) are found from subsection 7-1-1 and shown in Table 8.

Table 8. Geometrical and geo-mechanical parameters of the rock slope

| Parameters | $H$ | $\delta$ | $\varphi$ | $\theta$ | $\beta$  | $k$  | $t$  | $\sigma_t$ | $\gamma$             |
|------------|-----|----------|-----------|----------|----------|------|------|------------|----------------------|
| Units      | (m) | (Degree) | (Degree)  | (Degree) | (Degree) | ---- | (cm) | (MPa)      | (KN/m <sup>3</sup> ) |
| Values     | 8.5 | 55       | 10        | 100      | 30       | 0.5  | 35   | 2.3        | 23                   |

Substituting these parameters in Equation (7), the equivalent length of this slope was found to be 3.29 m. Hence, the safety factor of the slope against block-flexural toppling failure can be found with the modeling of two blocks with a length of 3.29, as shown in Figure 19. Therefore, using Equation (10), we can find its safety factor against block-flexure toppling failure as follows.

$$F_{SBF} = 0.5 \times \frac{0.33}{3.29 \times \tan 55} + (1 - 0.5) \frac{0.33 \times 2300}{33.29^2 \times 23 \times \cos 55} = 0.974 \quad (11)$$

As shown, the safety factor of this slope is nearly equal to 1 which conforms very satisfactorily to reality, because this slope is on the limit equilibrium condition and its safety factor should be equal to 1.

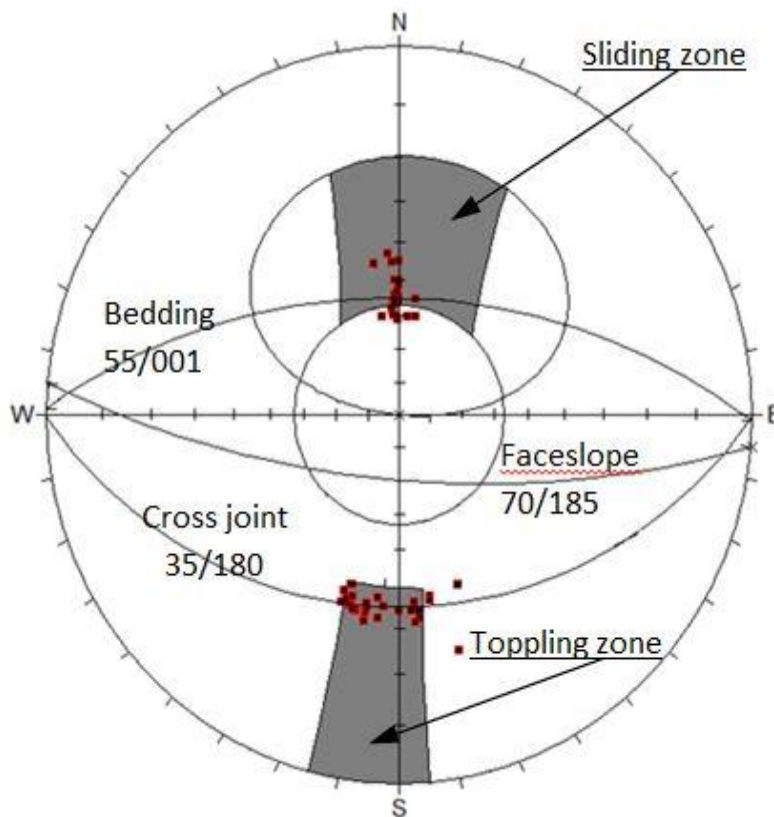


Fig. 18. Kinematic stability analysis of the case study slope

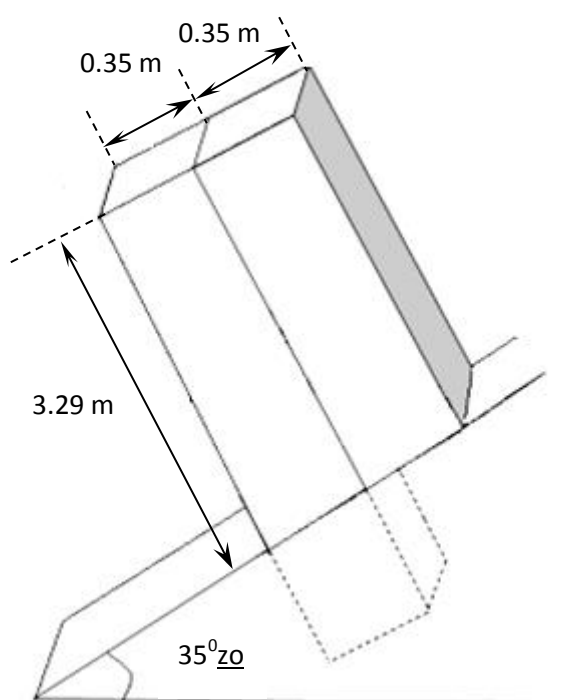


Fig. 19. Modeling of rock slope with a potential of block-flexure toppling failure with two equivalent columns

## 9. Conclusions

In this research, a special chemical powder was used to prepare synthetic solid blocks. The powder was turned, under a consolidation pressure of 210 kPa, into blocks 2.34 gr/cm<sup>3</sup> in density, and 56.7 kPa in compressive strength. Since, on the one hand, the blocks' tensile strengths are quite low and, on the other hand, this parameter highly affects the block-flexure toppling failure, to determine the tensile strength of the blocks, a special apparatus was designed and constructed; using this device, the blocks' tensile strength was found to be 32.37 kPa. The solid blocks were used to make several physical models of rock slopes with a potential of block-flexure toppling failure, and their failure was studied using the tilting table. Then, a theoretical method was proposed for the stability analyses of rock slopes against such failures. Based on the proposed method, it is possible to directly find the safety factor of such slopes. A comparison of the results of this method with those found from physical models shows that the suggested theoretical approach is appropriate for the analysis of such failures. Also, for the practical verification of the results of the theoretical approach, a case study was

evaluated using this method. The results found from the analyses of the case study have verified the correctness of the results of the proposed method.

## Acknowledgements

The authors express their sincere thanks to Prof. Ömer Aydan from the University of Ryukyus, Okinawa, Japan for his invaluable help and guidance.

## References

- [1] Müller, L. (1968). New considerations on the Vaiont slide. *Rock MechEngGeol*, 6:1-91.
- [2] Ashby, J. (1971). Sliding and toppling modes of failure in models and jointed rock slopes. M Sc thesis Imperial College University of London.
- [3] Turner, AK., Schuster, RL. (1996). *Landslides. Investigation and mitigation*. National Academy Press.
- [4] Choquet, P., Tanon, DDB. (1985). Nomograms for the assessment of toppling failure in rock slopes. 26th US Symposium on Rock Mechanics Rapid City, 19-30.
- [5] Hoek, E., Bray, J. (1977). *Rock Slope Engineering*. 1st edn IMM London.



- [6] Zambak, C. (1984). Design charts for rock slopes susceptible to toppling. *Geotechnical Engineering*, Vol. 109, No. 8, 1039-1062.
- [7] Goodman, RE., Bray, JW. (1976). Toppling of rock slopes. *ASCE Specialty Conference on Rock Engineering for Foundations and Slopes Boulder Colorado*, 2:201-234.
- [8] Wyllie, DC. (1980). Toppling rock slope failures examples of analysis and stabilization. *Rock Mech*, 13(2): 89-98.
- [9] Aydan, Ö. (1989). The stabilisation of rock engineering structures by rockbolts. Doctorate Thesis, Nagoya University, 204 pages.
- [10] Aydan, Ö., Kawamoto, T. (1992). Stability of slopes and underground openings against flexural toppling and their stabilization. *Rock Mech Rock Engng*, 25(3):143-165.
- [11] Bobet, A. (1999). Analytical solutions for toppling failure (Technical Note). *Int J Rock Mech MinSci*, 36: 971-80.
- [12] Sageseta, C., Sanchez, JM., Caizal, J. (2001). A general solution for the required anchor force in rock slopes with toppling failure. *Int J Rock MechMin.Sci*, 38:421-35.
- [13] Adhikary, DP., Dyskin, AV., Jewell, RJ., Stewart, DP. (1997). A Study of the Mechanism of Flexural Toppling Failure of Rock Slopes. *Rock Mech Rock Engng*, 30(2):75-93.
- [14] Adhikary, DP., Guo, H. (2002). An orthotropic Cosserat elasto-plastic model for layered rocks. *Rock Mech Rock Engng*, 35(3):161-170.
- [15] Amini, M., Majdi, A., Aydan, Ö. (2008). Stability Analysis and the Stabilization of Flexural Toppling Failure. *Rock Mech Rock Engng*, 42(5):751-782.
- [16] Amini, M. (2009). Dynamic and static slope stability analysis and stabilization of flexural toppling failure (Theoretically, experimentally and case histories). Ph.D. thesis, University of Tehran, Tehran, Iran.
- [17] Aydan, Ö., Amini, M. (2009). An experimental study on rock slopes against flexural toppling failure under dynamic loading and some theoretical considerations for its stability assessments. *the school of marine science and technology Tokai university*, 7(2): 25-40.
- [18] Amini, M., Majdi, A., Veshadi, MA. (2012). Stability analysis of rock slopes against block-flexure toppling failure. *Rock Mechanics and Rock Engineering*, 45(4):519-532.
- [19] Brideau, M., Stead, D. (2009). Controls on block toppling using a three dimensional distinct element approach. *Rock Mech Rock Engng*, DOI 10.1007/s00603-009-0052-2.
- [20] Majdi, A., Amini, M. (2010). Analysis of geo-structural defects in flexural toppling failure. *In J Rock Mech Min Sci*, 48(2):175-186.
- [21] Brideau M-A, Stead D (2009) Controls on block toppling using a three-dimensional distinct element approach. *Rock Mech Rock Eng* 43:241-260.
- [22] E. Mohtarami E., Jafari A. and Amini M. (2014) Stability analysis of slopes against combined circular-toppling failure. *International Journal of Rock Mechanics & Mining Sciences* 67 (2014) 43-56.
- [23] Amini M. and Akbarpour T. (2014) stability analysis of rock slopes facing dam lakes against block toppling failure. *Iranian Journal of mining engineering*, Vol. 9, No. 22, 52-64.
- [24] Alejano, L.R., Carranza-Torres, C., Giani, G.P., Arzua, J. (2015). Study of the stability against toppling of rock blocks with rounded edges based on analytical and experimental approaches. *Engineering Geology* 195, 172-184.
- [25] Egger, P. (1983). A new development in the base friction technique. *CollPhysGeomech Models ISMES*, 67-87, Bergamo.
- [26] Altaee, A., Fellenius, BH. (1994). Physical modeling in sand. *Can Geotech J* 1994; 31: 420-431.